Available online at www.sciencedirect.com
SCIENCE DIRECT®
Journal of Inorganic Biochemistry 98 (2004) 995–1001
Journal of Inorganic Biochemistry
www.elsevier.com/locate/jinorgbio

New solid state Ni(II)-famotidine square-planar complex: powder diffraction and spectroscopic studies

Malgorzata Baranska [a,*], Wiesław Łasocha [a], Henryk Kozłowski [b], Leonard M. Proniewicz [a,c,*]

[a] *Faculty of Chemistry, Jagiellonian University, 3 Ingardena Str., 30-060 Kraków, Poland*
[b] *Faculty of Chemistry, University of Wrocław, 14 F. Joliot-Curie Str., 50-383 Wrocław, Poland*
[c] *Laser Raman Laboratory, Regional Laboratory of Physicochemical Analysis and Structural Research, Jagiellonian University, 3 Ingardena Str., 30-060 Kraków, Poland*

Received 13 August 2003; received in revised form 11 February 2004; accepted 17 February 2004
Available online 19 March 2004

Abstract

Recent potentiometric studies have claimed that Ni(II) forms three pH-dependent complexes with famotidine. We isolated two of them from the solution; namely the paramagnetic complex NiL with octahedral geometry and the diamagnetic complex $NiH_{-2}L$ with square-planar geometry. The latter compound constitutes the subject of this work.

The crystal structure of nickel (II) famotidine complex $NiC_8N_7O_2S_3H_{13}$ discussed here, determined with the powder diffraction method, has shown that it belongs to a *Pbcn* space group (60) with *a*, *b*, *c* = 24.328(4), 14.747(2), 7.786(1), $V = 2793.6(5)$ Å^3. R_F and R_{wp} are 16.1% and 15.5%, respectively. Additionally, the UV–VIS, FT-FIR and Raman spectroscopic methods were employed to discuss and support the structure of the $NiH_{-2}L$ complex suggested by X-ray data.

The structure presented in this work is the second example of the complex of a famotidine ligand with a transition metal ion in the solid state. The other one, reported from a single crystal X-ray structure of famotidine complex with Cu(II), is quite different.

Keywords: Ni(II)-famotidine complex; Powder diffraction method; Rietveld method; UV–visible; FT-FIR; Raman spectroscopy

1. Introduction

Famotidine (**fam**), 3-[[[2-[(aminoiminomethyl)amino]-4-thiazolyl]methyl]thio]-*N*-(aminosulfonyl) (Fig. 1), is a histamine H_2-receptor antagonist that is a high potent inhibitor of gastric and acid secretion in humans [1,2]. It has been used mainly for the treatment of peptic ulcers and the Zollinger–Ellison syndrome. Due to the presence of amino, amido and thioether groups in its structure, this drug possesses chelating properties and may interact very effectively with the essential metal ions present in blood plasma and different tissues. Transition metal famotidine complexes have been recently investigated in view of their potent biological activity involving such metal ions as Cu(II), Ni(II), Pt(II) and Pd(II) [3–8].

The Cu(II)-famotidine complex was obtained and its crystal structure determined using the single crystal X-ray method [4]. The data show that Cu(II) coordinate to a **fam** molecule through guanidine N(3), thiazole N(9) nitrogen atoms, tioether sulfur S(11) from the aliphatic chain and a terminal amidine nitrogen N(16) atom. Recently, a new complex, $NiH_{-2}L$, consisting of famotidine with the Ni(II) ion has been reported in the solid state obtained at pH 8. This complex appeared to be diamagnetic [5]. Unfortunately, due to the lack of suitable single crystals, its molecular structure was proposed mainly based on IR and RS spectra in the solid state and on the ^{15}N, ^{13}C, ^{1}H NMR measurements in the DMSO (dimethyl sulfoxide) solution. These data confirmed square-planar geometry of the discussed complex, in which two protons were released from a ligand to form $NiH_{-2}L$ without the anion

* Corresponding authors. Tel.: +48-12-633-6377; fax: +48-12-634-0515 (M. Baranska).
E-mail addresses: baranska@chemia.uj.edu.pl (M. Baranska), proniewi@chemia.uj.edu.pl (L.M. Proniewicz).

0162-0134/$ - see front matter © 2004 Elsevier Inc. All rights reserved.
doi:10.1016/j.jinorgbio.2004.02.016

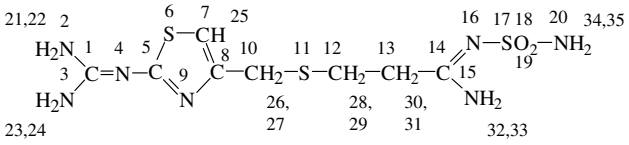

Fig. 1. Atom numbering of molecule of famotidine.

participation in the molecular structure. This means that the counter anion from the $Ni(ClO_4)_2$ salt used to prepare the Ni-**fam** complex is absent, which was additionally supported by the lack of the characteristic perchlorate vibrations in the Raman and IR spectra. The NMR data led us to the suggestion that four nitrogen donors: N(3), N(9), N(15) and N(20) of **fam** coordinate to Ni(II), forming a complex with square-planar geometry [5]. However, it turns out that the Ni(II)-**fam** complex takes on a different structure in the DMSO solution and in the solid state when precipitated from the aqueous solution.

This work presents the crystal structure of a new $NiH_{-2}L$ complex in the solid state. Its structure is determined with the powder diffraction method. Additionally, the UV–visible, FT-FIR and Raman spectra of this compound are discussed to support the structure proposed.

2. Experimental

2.1. Preparation of compound

Famotidine of the highest grade was donated by the "Polfa" Pharmaceutical Co. (Starogard Gdañski, Poland) and used without further purification. The $NiH_{-2}L$ complex was prepared following the procedure described in literature [5]. Briefly, the Ni(II)-**fam** complex was synthesized by adding the $Ni(ClO_4)_2$ aqueous solution dropwise to hot (80 °C) famotidine solution stirred vigorously until the metal to ligand ratio reached 1:1. The pH of the solution was controlled and adjusted with 0.01 M NaOH to the value of 8. The yellow microcrystalline powder precipitated was collected, washed twice with cold water and completely dried in desiccator over P_2O_5.

The Ni(II) to **fam** ratio was confirmed to be 1:1 by the elemental analysis and mass spectrometry (calc. C: 24.4, H: 3.3, N: 24.9; found: C: 24.4, H: 3.2, N: 24.5).

2.2. X-ray measurement

The details of the data collection are presented in Table 1. The diffraction pattern was indexed in the orthorhombic system using a program written by Visser [9]. Additionally, the measurements were repeated twice for two freshly obtained complexes. These two independent X-ray measurements show almost ideal agreement between the diffraction patterns obtained. After refining the lattice constants using the PROSZKI system [10], the space group *Pbcn* (60) for the Ni-**fam** complexes investigated was found by the systematic absence analysis. The list of powder diffraction lines was sent to ICDD to be included in the PDF-2 file.

Table 1
Details of data collection, crystal structure solution and refinement for Ni(II) famotidine complex

Diffractometer	PW3710 Philips X'pert PRO
Radiation	Cu K_α, graphite monochromator
2θ range	5–84
Step scan increment, count time (°, s)	0.02, 12
Standard peak: hkl, 2θ[a]	2 0 0, 12.003
hkl index range	0–13, 0–7, 0–22
R for standard peak (%)	2.2
Space group	*Pbcn* (60)
a (Å)	24.328 (4)
b (Å)	14.747 (2)
c (Å)	7.786 (1)
V (Å)	2793.6 (5)
Program used for structure solution	EXPO [18], FOX [19]
Structure refinement	XRS82 [20]
Number of observations	4450
Number of reflections	1246
Total number of atoms	21
Number of structural parameters refined	65
Number of profile parameters refined	9
Number of constraints	24 distances, 29 angles
R_F	16.1
R_{wp}	15.5
Maximum shift/error	0.05
Texture correction formula	exp(Gcos2α)
Preferred orientation vector and factor G	[0 1 0], 0.20(2)

[a] In XRS82 so called 'learned' peak shape is used. Selected by user standard peak is decomposed into set of base functions. These functions in tabulated form are used next by profile fitting procedure.

2.3. Spectroscopic measurements

The UV–visible absorption spectra of famotidine and Ni(II)-famotidine complex dissolved in DMSO (dimethyl sulfoxide) were recorded using the standard procedure. The UV–visible reflectance spectra were measured in $BaSO_4$ pellets versus $BaSO_4$ as a reference. The spectra were collected on a Shimadzu spectrometer model 2101 PC equipped with an ISR-260 attachment.

The FT-FIR spectrum was recorded in a low molecular weight polyethylene disc. 512 scans were collected, with resolution set at 2 cm^{-1}. The FT-FIR spectrum was measured with a Bio-Rad spectrometer model FTS 60V. The accuracy of frequency reading was ± 1 cm^{-1}.

The Raman measurement was taken at room temperature by exposing the complex obtained to the 514.5 laser line from a Spectra-Physics model 2025. The laser power at the sample was maintained at 20 mW. Raman spectrum was collected on a Spex model 1403 Czerny–Turner double monochromator equipped with a Hamamatsu R928 photomultiplier. The DM1B spectroscopy lab coordinator was used to control data acquisition. The spectral band-pass was set at 4 cm^{-1}. Eight scans were collected for the complex. The accuracy of frequency reading was ± 1 cm^{-1}.

2.4. Calculations

The calculation were carried out at the density functional theory level (DFT), using the B3LYP [6,7] exchange-correlation functional implemented in the Gaussian '98 program [11]. This method is recommended by Scott and Radom [12], and yields one of the best agreements between the experimental and calculated frequencies. The calculations were performed with the LanL2DZ basis set [13] which included some relativistic effects. This method is recommended for calculations of metal complexes. The application of this basis provides the D95V basis set for ligand elements and a double-zeta basis set containing effective core potential (ECP) representations of core electrons for the nickel ion.

In the beginning, geometry optimization of $NiH_{-2}L$ was conducted, and followed by frequency calculations. No imaginary frequencies at equilibrium geometry were found. The GAR2PED Program [14] was used to calculate the potential energy distribution (PED) of normal modes.

3. Results and discussion

3.1. UV–VIS spectroscopy

Our earlier studies of the diamagnetic Ni(II)-**fam** complex showed that the ligand undergoes a two-proton dissociation process upon complex formation in the solution, as well as in the solid state [5]. A similar pattern (in the solution) has been observed for some peptide ligands when a planar complex is formed with a simultaneous release of two or three protons [15,16]. The FT-Raman and FT-IR spectra of this Ni(II)-**fam** complex in the solid state show a lack of characteristic perchlorate anion vibrations. On the other hand, the integration of the ^1H NMR spectra of Ni(II)-**fam** in the DMSO solution resulted in 13 protons. This confirms the loss of two protons from the **fam** ligand upon its coordination to Ni(II) [17]. Additionally, undisputable ^{13}C and ^{15}N NMR spectra have led us to the conclusion that the diamagnetic Ni(II)-**fam** complex obtained in the DMSO solution is tetragonal, with **fam** coordinated to the nickel (II) ion by four nitrogen donors: N(3), N(9), N(16) and N(20). At that time, the involvement of S(11) in the complex seemed to be less favoured and, in fact, no characteristic $S \rightarrow Ni(II)$ charge transfer band was observed in the electronic absorption UV–visible spectrum (in the aqueous solution) [1,5].

Fig. 2 presents the UV–visible spectra of **fam** and its Ni(II) complex in the solid state as well as in the DMSO solution measured in the 220–360 nm range. The spectra of free **fam** (Fig. 2(a)) and those of its complex with Ni(II) in DMSO (Fig. 2(b)) show a maximum at the same wavelength (295 nm). This band is probably a consequence of the electronic transition within the thiazole ring, confirming our earlier report, in which the thiazole sulphur atom was not involved in the Ni(II)-**fam** complex formed in the DMSO solution. A similar absorption band is observed for **fam** in the solid state measured with the reflectance technique (Fig. 2(c)). However, the reflectance spectrum of the Ni(II)-**fam** complex (Fig. 2(d)) shows several bands with the most pronounced absorption with a maximum at 327 nm. This absorption band

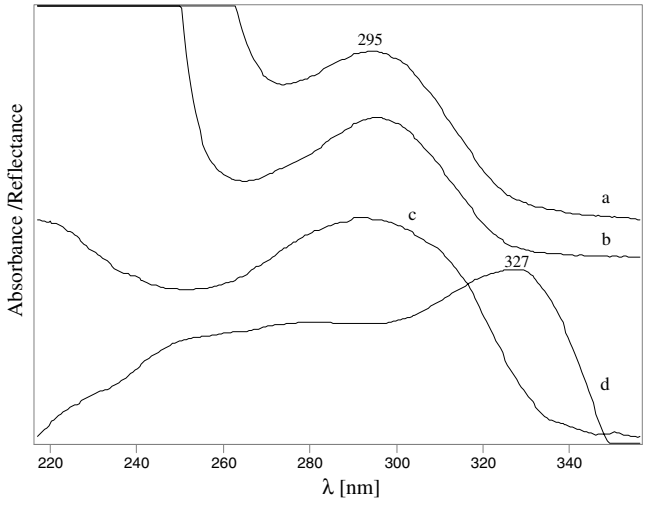

Fig. 2. UV–visible spectra of (a) famotidine in DMSO, (b) Ni(II)-famotidine complex in DMSO, (c) famotidine in solid state, (d) Ni(II)-famotidine complex in solid state.

can be assigned to a weak S → Ni(II) charge transfer transition originating not from the thiazole but from the thioether atom. The comparison of the Ni(II) complex spectrum in the DMSO solution and in the solid state clearly indicates the formation of a new Ni(II)-**fam** tetragonal complex. In other words, the coordination of a nickel ion engages other donors of **fam** in the solid state than in the DMSO solution.

It has to be mentioned that in the visible range (data not shown) two absorptions are observed for the discussed solid state Ni(II)-**fam** complex at 430 and 515 nm. With no doubts, these bands are due to the Ni(II) d–d transitions of the planar complex. Similarly, the square planar Ni(II)-**fam** complex obtained in the aqueous solution shows two transitions at 417 and 505 nm [1]. These data are almost identical with those obtained for the DMSO solution. These d–d transitions cause that the discussed compounds are yellow. It has to be emphasized that the octahedral Ni(II)-**fam** complex (blue colour) exhibits drastically different UV–VIS spectrum [1].

3.2. Crystal structure solution and refinement

The initial structure model was built independently using two methods. First, we tried to solve the solid state structure ab initio using the EXPO program [18]. Since the proposed model was slightly different from that suggested previously [5], and very difficult to refine and complete with the Rietveld method, we decided to apply the so-called direct space methods using the FOX program [19]. In this approach, the famotidine molecule was coordinated to Ni(II) by two nitrogen atoms, N3 and N9, only (see Fig. 3), while the other part of the ligand was allowed to vary. Despite many trials and different starting points, the global optimization procedure always resulted in the structure presented in Fig. 3. This structure was additionally refined with the Rietveld model using the XRS-82 program [20,21].

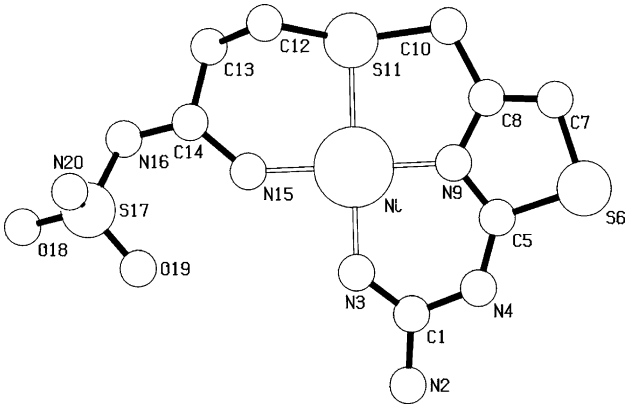

Fig. 3. Molecular structure of Ni(II)-famotidine square-planar complex with numbering scheme.

The temperature factors could not be refined for all atoms individually, hence they were divided into a few groups. Their B factors were constrained to be equal to each other during refinement. In this way, all B factors were refined to positive values without increasing the R_F and R_{wp} values. This methodology introduced some differences between the patterns observed and those calculated, particularly in the 2Θ range, close to the two strongest diffraction peaks in the obtained patterns. Obviously, this was caused by the limitation of the XRS-82 program while describing the peak shape, since that program uses only one peak shape function for all peaks in the pattern.

In this work, the initial structure of the complex, found by direct methods, was difficult to refine and complete using the Rietveld method. Thus, we decided to determine it using the "direct space" global optimization technique. It is evident from the data presented here that, for structure complexity of about 20 non-H atoms in the asymmetric unit, it is possible to solve this crystal structure ab initio using powder diffraction data without any commercially available software for the global optimization procedure, even if the exact molecular structure is unknown.

3.3. Structure description and discussion

The Ni(II)-**fam** square-planar complex structure along with its numbering scheme is presented in Fig. 3. Fig. 4 shows molecular packing along [0 1 0] (note that the **a**-axis is oriented upwards). The dashed lines indicate intermolecular H-bonds. The atomic coordinates and the selected bond distances are listed in Tables 2 and 3, respectively. The coordination polyhedron of nickel (II), which indicates a distorted square-planar structure, consists of three nitrogen atoms and one sulphur atom, namely N(3), N(9), N(15) and S(11). As shown in Fig. 4, the isolated, puckered molecules perpendicular to the b axis form columns parallel to direction [0 1 0]. In such structure, the closest Ni–Ni distance is 3.90 Å. In short, 16 of the **fam**'s non-H atoms are involved in a tetrad-

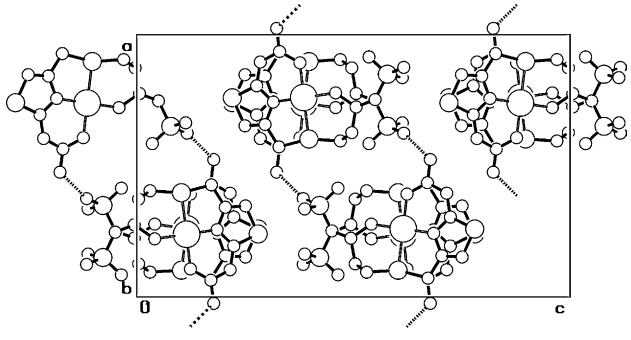

Fig. 4. Drawing of the molecular packing along [0 1 0] of Ni(II)-famotidine complex (an **a**-axis is oriented upwards). Dashed lines indicate intermolecular H-bonds.

Table 2
Atomic coordinates and isotropic temperature factors[a]

Atom	*x*	*y*	*z*	*U*
Ni	0.2394(9)	0.274(2)	0.6148(5)	0.039(6)
C1	0.064(1)	0.298(4)	0.671(1)	0.011(6)
N2	−0.024(2)	0.260(7)	0.677(2)	0.01121
N3	0.107(2)	0.293(5)	0.6235(8)	0.01121
N4	0.104(2)	0.370(5)	0.715(1)	0.01121
C5	0.195(1)	0.379(5)	0.7236(8)	0.01121
N6	0.257(1)	0.370(5)	0.685(1)	0.01121
S7	0.241(2)	0.492(4)	0.7798(9)	0.01742
C8	0.347(2)	0.48(1)	0.751(2)	0.01121
C9	0.342(1)	0.392(8)	0.704(1)	0.01121
C10	0.428(1)	0.35(1)	0.672(2)	0.01121
S11	0.398(1)	0.268(3)	0.6028(9)	0.017(6)
C12	0.405(2)	0.285(4)	0.530(1)	0.01121
C13	0.373(2)	0.121(5)	0.504(1)	0.01121
C14	0.276(1)	0.130(3)	0.4939(8)	0.01121
N15	0.222(1)	0.165(6)	0.541(1)	0.01121
N16	0.248(2)	0.049(3)	0.450(1)	0.01121
S17	0.1509(9)	0.101(2)	0.4218(8)	0.01742
O18	0.125(2)	−0.033(6)	0.384(2)	0.0824
O19	0.085(2)	0.127(6)	0.464(1)	0.0824
N20	0.164(3)	0.282(6)	0.387(2)	0.08(3)

[a] The e.s.d of the last significant digit is given in parentheses. The e.s.d's were calculated according to Scott [22].

Table 3
Selected bond lengths (Å)

Atom 1–atom 2	Experimental bond (e.s.d)	Calculated (B3LYP/Lanl2dz)
Ni–N3	1.97 (3)	1.89
Ni–N9	1.88 (3)	1.89
Ni–S11	2.35 (2)	2.30
Ni–N15	1.99 (3)	1.88

entate square planar complex with nickel, while the remaining SO_2–NH_2 pendant arm participates in the intermolecular hydrogen bonding in the solid state. Fig. 5. presents the calculated (upper), observed (middle) and difference (lower) Rietveld profiles.

A comparison of the quantum-chemical calculation of Ni(II)-**fam** complex geometry in the DMSO solution with that obtained in the solid state leads to the following conclusions. The calculated energies of equilibrium geometry for both nickel(II) complexes, i.e. those discussed in [5] and in this work, are almost identical with the solid state complex energy higher by $\Delta E = 0.225$ kcal mol^{-1} in comparison to that for the complex in DMSO solution. A transformation of the Ni(II)-**fam** complex from the solution to the solid state is accompanied by the breaking of two Ni–N bonds, i.e. Ni–N16 (1.99 Å) and Ni–N20 (1.93 Å), to form new bonds: Ni–S11 (2.30 Å) and Ni–N15 (1.88 Å) (see Table 3). It has to be emphasized that a square-planar Ni-**fam** complex instantly precipitates after the aqueous solutions of Ni(II) salt is mixed with **fam**, whereas the complex obtained in DMSO does not precipitate at all. Thus, different physicochemical conditions are responsible for the formation of these two square-planar complexes with different **fam** arrangement around Ni(II).

It is worth noticing that three donors of **fam** to the nickel (II) ion are the same as for the copper (II) ion in the solid state, namely: N(3), N(9) and S(11). The last bonding site is occupied by nitrogen N(15) for Ni(II) and N(16) for Cu(II). Such binding enforces a different arrangement of the tail of the famotidine ligand in both complexes. It should be mentioned that a similar coordination pattern (N, N, N, S) is observed for other diamagnetic Ni(II) complexes in the solid state [23].

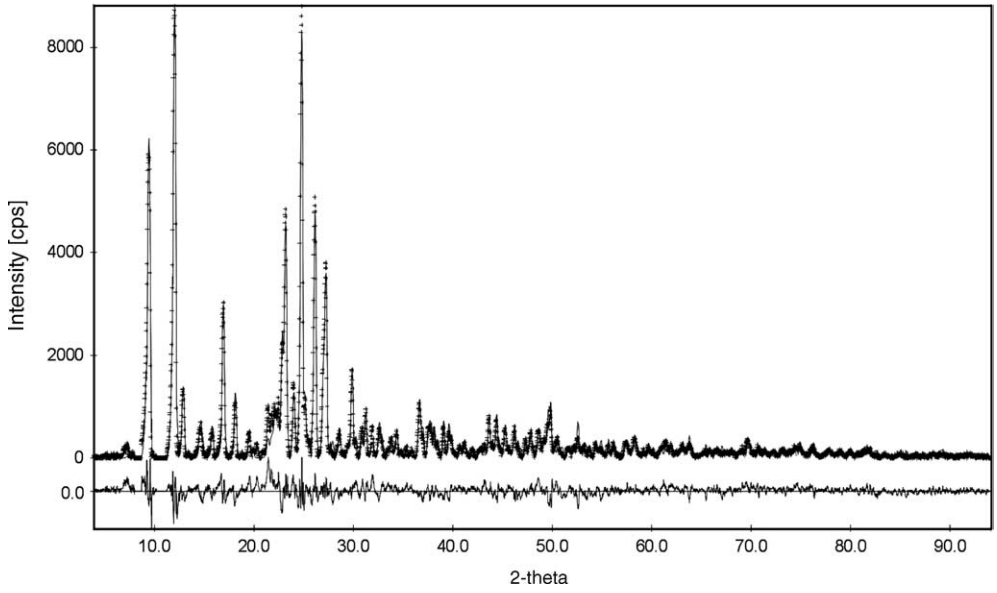

Fig. 5. Calculated (solid), observed (crosses) and difference (lower) Rietveld profiles.

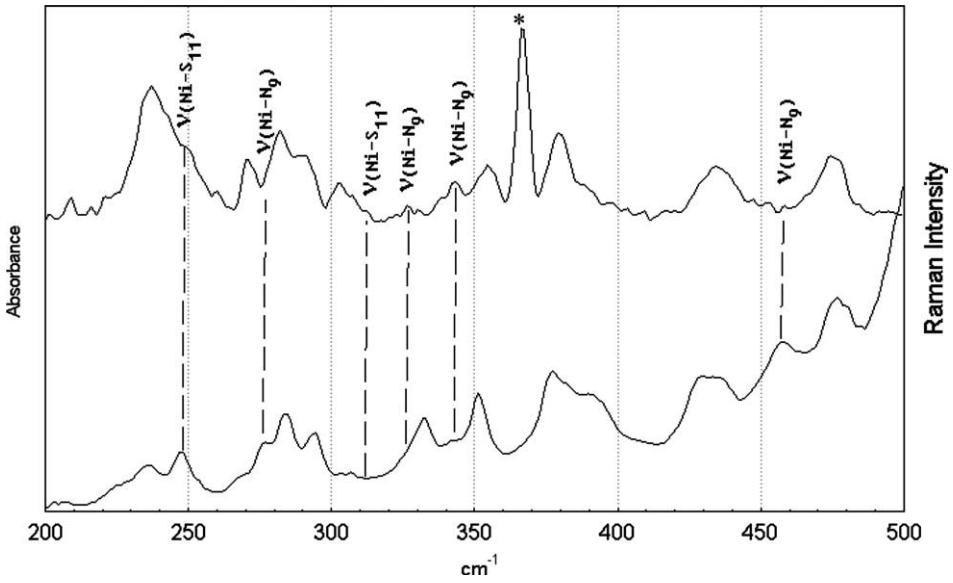

Fig. 6. FT-Raman (upper) and FT-FIR (bottom) spectra of Ni(II)-famotidine complex in solid state (* plasma line).

Two other **fam** complexes in the solid state have been reported in literature with Pt(II) and Pd(II) ions; however, they have not been characterized structurally. In the former case, three donors: N(3), N(9) and S(11) are engaged in the coordination of Pt(II), whereas the forth binding site is occupied by the anion [8]. In the latter, the Pd(II) ion is bonded by thiazole nitrogen N(9), thioether sulphur S(11) and two coordinated anions [8].

3.4. Vibrational spectra of Ni(II)-*fam* in the solid state

The FT-FIR and Raman spectra of the discussed square-planar Ni(II)-**fam** complex in the solid state here are shown in Fig. 6. It is known that the low-frequency region provides information about the structure and bonding of the metal–ligand linkage [24]. However, in many cases metal–ligand vibrations can be masked by the deformation modes of the ligand itself [25].

In this work, we performed quantum chemical calculations to assign vibrational modes observed for the Ni(II)-**fam** complex in the range of 200–500 cm^{-1} (Table 4). This low frequency region differs substantially for the complex and the ligand itself. According to our calculations, a strong mixing of the ν(Ni–N), ν(Ni–S), δ(N–Ni–N) and δ(N–Ni–S) modes appears (see Table 4). Thus, this complicates clear observation of the Ni–ligand modes. For example, the stretching (Ni–N_9) mode contributes mainly to the bands at 457, 346, 326

Table 4
Vibrational bands assignment of Ni(II)-**fam** complex in the range 200–500 cm^{-1} based on calculations B3LYP/LanL2DZ

Experimental	Calculated	Assignment PED (%)
474	463	$\delta(N_{20}–H)(16) + \delta(S_{17}=O)(11)$
457	457	**ν(Ni–N_9)(15)** + δ(Ni–N_3)(11)
447	445	$\delta(N_2–H)(61) + \delta$(Ni–$N_3$)(21)
435	437	$\delta(N_{20}–H)(14) + \nu(N_{20}–S_{17})(11)$
420	418	$\delta(N_9–Ni–N_3,\ N_9–Ni–S_{11})(41) + \delta(N_{15}–Ni–N_3,\ N_{15}–Ni–S_{11})(10)$
388	385	$\delta(C_8–S_{11}–C_{10})(27)$
380	372	$\delta(N_3–Ni–S_{11},\ N_9–Ni–S_{11})(21) + \delta(C_8–S_{11}–C_{10})(15)$
355	357	$\delta(N_3–Ni–S_{11},\ N_9–Ni–S_{11})(52) + \delta$(Ni–$N_3$)(11)
343	346	**ν(Ni–N_9)(43)** + $\delta(N_9–Ni–N_3,\ N_9–Ni–S_{11})(12) + \delta(N_{20}–H)(10)$
332	326	**ν(Ni–N_9)(19)** + $\delta(N_9–Ni–N_3,\ N_9–Ni–S_{11})(13) + \delta(N_{20}–H)(12)$
312	313	$\delta(N_9–Ni–N_3,\ N_9–Ni–S_{11})(16) +$ **ν(Ni–S_{11})(15)** + $\delta(N_9–Ni–N_3,\ N_3–Ni–S_{11})(10)$
302	301	$\delta(N_9–Ni–N_3,\ N_9–Ni–S_{11})(24) + \delta(N_{15}–Ni)(18) + \delta(N_9–Ni–S_{11},\ N_3–Ni–S_{11})(12)$
294	298	$\delta(N_9–Ni–N_3,\ N_9–Ni–S_{11})(31) + \delta(N_{15}–Ni)(13) +$ **ν(Ni–N_9)(12)**
276	277	**ν(Ni–N_9)(25)** + $\delta(N_9–Ni–N_3,\ N_9–Ni–S_{11})(25)$
273	275	$\delta(N_9–Ni–N_3,\ N_9–Ni–S_{11})(52) + \delta(C_8–S_{11}–C_{10})(27)$
260	263	$\delta(N_9–Ni–S_{11},\ N_3–Ni–S_{11})(49) + \tau$ ring
248	249	$\delta(N_9–Ni–N_3,\ N_9–Ni–S_{11})(39) +$ **ν(Ni–S_{11})(34)**
221	219	$\delta(N_{15}–Ni)(32) + \delta(N_9–Ni–N_3,\ N_9–Ni–S_{11})(21)$
209	210	$\delta(N_9–Ni–N_3,\ N_9–Ni–S_{11})(41) + \delta(N_9–Ni–S_{11},\ N_3–Ni–S_{11})(18)$

and 277 cm^{-1}, whereas $\nu(Ni–S_{11})$ is observed at 313 and 249 cm^{-1}. On the other hand, the $\nu(Ni–N_3)$ and $\nu(Ni–N_{15})$ vibrations are distributed among several other modes with their contributions less than 10% of PED. Therefore, Table 4 has been included to illustrate the complexity of these vibrations, rather than proposing detailed vibrational band assignments for them.

4. Conclusions

The data presented indicate that the structure of the tetragonal Ni(II)-**fam** complex in the DMSO solution differs substantially from the complex obtained in the solid state from the aqueous solution. This structure shows some similarities to other solid state **fam**-M(II) complexes. For example, in the Cu(II) complex the N(3), N(9), N(16) and S(11) atoms are involved in metal ion binding, whereas the N(3), N(9) and S(11) atoms are engaged in the Pt(II) coordination.

Powder diffraction data show indisputably that Ni(II) coordinates to the **fam** molecule through the guanidine N(3), thiazole N(9), terminal amidine nitrogen N(15) and thioether sulfur S(11) atoms. However, other methods show [5] that when the complex is formed in the DMSO solution (or dissolved in it!) it provides exclusively four nitrogen donors: N(3), N(9), N(16) and N(20) of **fam** as a potential binding site for the nickel (II) ion, i.e. thioether sulphur atom is immediately replaced by N(20), thus ''reshaping'' the structure.

References

[1] H. Kozłowski, T. Kowalik-Jankowska, A. Anouar, P. Decock, J. Spychala, J. Świątek-Kozłowska, M.L. Ganadu, J. Inorg. Biochem. 48 (1992) 233.
[2] C.R. Ganellin, M.E. Parsons, Pharmacology of Histamine Receptors, J. Wright and Sons, Bristol, 1982.
[3] A.M. Duda, T. Kowalik-Jankowska, H. Kozlowski, T. Kupka, J. Chem. Soc. Dalton Trans. (1995) 2909.
[4] M. Kubiak, A.M. Duda, M.L. Ganadu, H. Kozlowski, J. Chem. Soc. Dalton Trans. (1996) 1905.
[5] M. Barańska, E. Gumienna-Kontecka, H. Kozłowski, L.M. Proniewicz, J. Inorg. Biochem. 92 (2002) 112.
[6] V. Nurchi, F. Cristiani, G. Crisponi, M.L. Ganadu, G. Lubini, A. Panzanelli, L. Naldini, Polyhedron 11 (21) (1992) 2723.
[7] G. Crisponi, F. Cristiani, V.M. Nurchi, R. Silvagni, M.L. Ganadu, G. Lubinu, L. Naldini, A. Panzanelli, Polyhedron 14 (11) (1995) 1517.
[8] G.B. Onoa, V. Moreno, J. Inorg. Biochem. 72 (1998) 141.
[9] J.W. Visser, J. Appl. Cryst. 2 (1969) 89.
[10] W. Łasocha, K. Lewinski, J. Appl. Cryst. 27 (1994) 437.
[11] M.J. Frisch, G.W. Trucks, H.B. Schlegel, G.E. Scuseria, M.A. Robb, J.J.R. Cheeseman, V.G. Zakrzewski, J.A. Montgomery, R.E. Stratmann, J.C. Burant, S. Dapprich, J.M. Millam, A.D. Daniels, K.N. Kudin, M.C. Strain, O. Farkas, J. Tomasi, V. Barone, M. Cossi, R. Cammi, B. Mennucci, C. Pomelli, C. Adamo, S. Cliffird, J. Ochterski, G.A. Petersson, P.Y. Ayala, Q. Cui, K. Morokuma, D.K. Malick, A.D. Rabuck, K. Raghavachari, J.B. Foresman, J. Ciosłowski, J.V. Ortiz, B.B. Stefanov, G. Liu, A. Liashenko, P. Piskorz, I. Komaromi, R. Gomperts, R.L. Martin, D.J. Fox, T. Keith, M.A. Al-Laham, C.Y. Peng, A. Nanayakkara, C. Gonzalez, M. Challacombe, P.M.W. Gill, B.G. Johnson, W. Chen, M.W. Wong, J.L. Andres, M. Head-Gordon, E.S. Replogle, J.A. Pople, Gaussian 98 (Revision A.1), Gaussian, Inc, Pittsburgh PA, 1998.
[12] A.P. Scott, L. Radom, J. Phys. Chem. 100 (1996) 16502.
[13] B. Foresman, A. Frisch, Exploring Chemistry with Electronic Structure Methods, Gaussian Inc, Pittsburgh, 1993.
[14] J.M.L. Martin, C. Van Alsenoy, Gar2ped, University of Antwerp, 1995.
[15] L.D. Pettit, J.E. Gregor, H. Kozłowski, in: R.W. Hay, J.R. Dilworth, K.B. Nolan (Eds.), Perspectives on Bioinorganic Chemistry, JAI Press, London, 1991, pp. 1–41.
[16] H. Sigel, R.B. Martin, Chem. Rev. 82 (1982) 385.
[17] M. Barańska, K. Czarniecki, L.M. Proniewicz, J. Mol. Struct. 563 (2001) 347.
[18] A. Altomare, M.C. Burla, G. Cascarano, C. Giacovazzo, A. Guagliardi, G.G. Moliterni, G. Polidori, J. Appl. Cryst. 32 (1999) 339.
[19] V. Favre-Nicolin, R. Cerny, J. Appl. Cryst. 35 (2002) 734.
[20] Ch. Baerlocher, XRS-82. The X-ray Rietveld system, Institut f. Kristallographie, ETH, Zurich, Switzerland, 1982.
[21] D. Mucha, W. Łasocha, J. Appl. Cryst. 27 (1994) 201.
[22] H.G.J. Scott, Appl. Cryst. 16 (1983) 159.
[23] N.C. Kasuga, K. Sekino, C. Koumo, N. Shimada, M. Ishikawa, K. Nomiya, J. Inorg. Biochem. 84 (2001) 55.
[24] M. Barańska, L.M. Proniewicz, J. Mol. Struct. 511 (1999) 153.
[25] K. Nakamoto (Ed.), Infrared and Raman Spectra of Inorganic and Coordination Compounds, V, John Wiley and Sons, New York, 1997.